https://doi.org/10.5194/wes-2024-189
Preprint. Discussion started: 15 January 2025

eawe european academy of wind energy
Open Access WIND ENERGY SCIENCE DISCUSSIONS

Comparative anomaly detection for floating offshore wind turbines using in-situ data.

Adrien Hirvoas[1], Cesar Aguilera[2], Matthieu Perrault[3], Damien Desbordes[3], and Romain Ribault[1]

[1]France Energies Marines, 525 Av. Alexis de Rochon, 29280 Plouzané
[2]SERCEL, 22 Rue des Platanes, 38120 Saint-Egrève
[3]SERCEL, 16 Rue du Bel air, 44470 Carquefou

Correspondence: Adrien Hirvoas (adrien.hirvoas@france-energies-marines.org)

Abstract. This study introduces a comparison between a kurtosis-analysis and a deep learning-based approaches for detecting anomalies of a floating offshore wind turbine. The study uses in-situ measurements from a 2.3 MW floating offshore wind turbine named Zefyros and deployed approximately 11 kilometers off the coast of Norway. The first method employs the statistical metric of kurtosis to detect anomalies within a signal by identifying variations in the signal distribution. The second method employs a deep-learning procedure based on an auto-encoder approach, which transforms inputs into a reduced-dimensional latent space and then uses the encoded information to produce outputs identical to the inputs. One month of SCADA and high frequency measurements obtained thanks to S-Morpho sensors were used in the study. Due to limitations in the accessible SCADA information, the anomaly scenario was simplified to detecting whether the turbine rotor was rotating or not. Both tested methodologies can accurately detect anomalies, with the ground truth based on rotor rotations per minute (rpm) measurements. The auto-encoder method shows promising results, delivering more accurate outcomes than the kurtosis analysis on this in-situ measurement dataset. This study is a first step toward a more general use of auto-encoders for wind turbine anomaly detection. The latent space build by the auto-encoder can be leveraged to detect other types of anomalies, with a few labeled data.

1 Introduction

The Floating Offshore Wind Turbine (FOWT) is a rapidly expanding form of renewable energy. However, as of 2021, only 113 MW were operational in Europe (Ren21, 2021). The noise and visual pollution controversies surrounding onshore wind turbines, coupled with the potential for increased energy production, have prompted governments and institutions to propose ambitious plans for offshore sector expansion (WindEurope, 2022). FOWT systems, due to their minimized visual impact, are designed to be larger than their onshore equivalents (Gorostidi et al., 2023). This results in a larger swept area in areas where wind speeds are already high. These factors collectively contribute to a power output increase. Despite these advantages, the high costs associated with floating wind farms render them not yet competitive compared to fixed structures. In that context, the levelized cost of energy (LCOE) for floating offshore wind ranges between 90 euros/MWh and 120 euros/MWh (Gourvenec, 2020). In particular, approximately one-third of these costs are attributed to operation and maintenance (O&M) and other related activities (Nava et al., 2019). Consequently, the cost-effectiveness of wind turbines is negatively impacted by such high

https://doi.org/10.5194/wes-2024-189
Preprint. Discussion started: 15 January 2025

eawe european academy of wind energy
Open Access WIND ENERGY SCIENCE DISCUSSIONS

O&M costs. In order to mitigate these costs, minimize unscheduled downtime, and ensure high availability of wind turbine assets, there is a significant demand for predictive maintenance tools and advanced anomaly detection methods.

Anomaly detection has been extensively researched across various domains and application areas. Numerous techniques have been developed for anomaly detection, falling into categories such as trending, clustering, normal behaviour modelling, damage modelling, and assessment of alarms and expert systems (Tautz-Weinert and Watson, 2017). Especially in the wind turbine field, several studies have been led to explore the application of Supervisory Control and Data Acquisition (SCADA) for detecting anomalies (Stetco et al., 2019; Tautz-Weinert and Watson, 2017; Cui et al., 2018; Gonzalez et al., 2018; Stetco et al., 2019; Barahona et al., 2017). A variety of data-driven methodologies, such as neural network procedures (Zaher et al., 2009; Bangalore and Tjernberg, 2015), Support Vector Machine (SVM) (Dhiman et al., 2021), have been employed for wind turbine condition monitoring, all based on SCADA data.

However, in situations where SCADA data is either scarce or noisy, it may be difficult to construct a deep learning procedure for detecting anomalous behavior of the asset. This study explores the potential of using high frequency in-situ data. In the following document, we delve into two distinct types of anomaly detection. Firstly, we examine a method that involves the manipulation and analysis of signals derived from magnetometers. This method aims to detect anomalies by identifying variations from the standard geomagnetic field. Notably, this method employs the statistical metric of kurtosis to detect anomalies within a signal by identifying variations in a distribution. Kurtosis provides a quantification of a distribution's shape by assessing the tails of the distribution in relation to its peak, thereby facilitating the recognition of outliers or unusual patterns in the data. Secondly, we suggest the application of deep learning techniques that utilize sophisticated neural network structures to autonomously learn and extract complex features from intricate data for the detection of anomalies within the data. In that context, autoencoders, a type of artificial neural network, have gained significant attention due to several advantages that are believed to be applicable to the wind energy sector. Primarily, autoencoders are used for unsupervised tasks, which do not require labelled data during training. In more advanced configurations, autoencoders have proven to be efficient when used on semi-supervised problems (Tautz-Weinert and Watson, 2017; Berahmand et al., 2024; Sae-Ang et al., 2022), where only a limited number of labelled anomaly data are available for the training dataset. This is a notable advantage for wind turbines, as extensive historical failure data are typically not available. Furthermore, autoencoders can serve as a dimensionality reduction method and facilitate feature extraction from normal behavior data, which can subsequently be used for data clustering or classification (Berahmand et al., 2024). The proposed strategy for anomaly detection involves initially modeling normal behavior and subsequently leveraging this understanding to identify potential anomalies (Schlechtingen et al., 2013; Schlechtingen and Santos, 2014; Schröder et al., 2022). Most of the anomaly detection approaches have traditionally been applied to univariate time series data. However, as data becomes increasingly high-dimensional, detecting anomalies may require joint modeling of interactions between multiple variables. For such complex scenarios, deep learning approaches, such as convolutional autoencoders offer distinct benefits. Convolutional autoencoders can capture intricate relationships and patterns within high-dimensional data, making them well-suited for anomaly detection tasks.

The remainder of the article is structured as follows. In Section 2, the mathematical description of the proposed methods for detecting anomalies are described. In Section 3 the detailed methodologies are applied to the in-situ data from an offshore

https://doi.org/10.5194/wes-2024-189
Preprint. Discussion started: 15 January 2025

eawe european academy of wind energy
Open Access WIND ENERGY SCIENCE DISCUSSIONS

wind turbine operating in the north sea. The resulting model performances in detecting operating and non-operating periods are shown based on a limited one-month dataset. In Section 4, conclusions of this study are drawn and future work is suggested.

2 Methodology

Anomaly detection involves initially developing a procedure to recognize normal patterns and then generating anomaly scores to identify unusual behavior in the asset. The signal analysis conducted hereafter relies on a noise-based detection method (Zhao et al., 2021) and a kurtosis procedure. Indeed, one way to identify intermittency is to determine the probability density function (PDF), looking at how it differs from a Gaussian shape and especially for the presence of enhanced high energy tails (Franco et al., 2021). In that context, the approach relies on a statistical tool to analyze characteristics of data. This kurtosis indicator refers to the tailedness of a distribution, and therefore, to the outlier occurrence. The kurtosis parameter, also known as the standardized fourth central moment of a distribution, can be defined as:

$$K(X) = \frac{\mathbb{E}[(X-\mu)^4]}{\sigma^4},$$

where μ and σ are respectively the mean and standard deviation of the studied data denoted by X.

As mentioned in (Wang et al., 2016), kurtosis based techniques are efficient methods for signal processing in the context of anomaly detection. In the wind turbine domain, the statistical approach is also used for detection of bearing failures, see (Elforjani and Bechhoefer, 2018). In our application, to determine the wind turbine state, a magnetic signal obtained from a magnetometer located close to the rotor-nacelle-assembly (RNA) was analyzed. Such sensors measure magnetic field for the three physical axes (x, y, z) in μT (micro Tesla). This field is sensitive to electromagnetic interference from sources other than Earth's magnetic force as the magnetic effects of electric currents or the presence of ferromagnetic materials.

The deep learning method discussed hereafter rely on autoencoder models, which consist of two components: an encoder that maps input data to a low-dimensional space, and a decoder that reconstructs the original input data from this lower-dimensional representation. By structuring the problem this way, the encoder learns an efficient compression function, allowing the decoder to successfully reconstruct the original data. Autoencoders are commonly used for dimensionality reduction or noise removal from images and data compression. The specific mapping learned by an autoencoder is tailored to the training data distribution, making it crucial for anomaly detection. When applying an autoencoder for anomaly detection, the general principle is to first model normal behavior and then generate an anomaly score for each new data sample. This approach follows a semi-supervised paradigm, leveraging both large amounts of unlabeled data and small amounts of labeled data. The autoencoder is a specific type of artificial neural network (ANN), see (Chen and Guo, 2023). This mathematical concept relies on an artificial neuron which is a function of several variables that performs the linear combination of its inputs by arbitrary weights. Let us consider, a d-dimensional parameter vector $\mathbf{x} = (x_1, \ldots, x_p)$ from the set $\mathcal{P}$ previously defined. A neuron operating on the vector $\mathbf{x}$ has p weights denoted ω_1 to ω_p representing the importance given to their respective input x_j. The output of the artificial neuron,

https://doi.org/10.5194/wes-2024-189
Preprint. Discussion started: 15 January 2025

eawe european academy of wind energy
Open Access WIND ENERGY SCIENCE DISCUSSIONS

noted $s \in \mathbb{R}$, is a real number obtained by weighted sum, such that:

$$s = \sum_{i=1}^{p} w_i x_i \cdot$$

This equation can also be represented in matrix form by the multiplication between the row vector $\boldsymbol{\omega}$ and the column vector $\mathbf{x}$:

$$s = \boldsymbol{\omega}^T \mathbf{x} = \begin{bmatrix} \omega_1 & \omega_2 & \dots & \omega_p \end{bmatrix} \begin{bmatrix} x_1 \\ x_2 \\ \vdots \\ x_p \end{bmatrix} \cdot$$

In general, an artificial neuron is equipped with a bias $b \in \mathbb{R}$ so that the modeled function is an affine function, that is, a linear function followed by a translation. This allows the neuron to not only scale inputs by weights, but also to shift (translate) the function. This makes the model more flexible and capable of representing more complex patterns. It is defined as:

$$s = \boldsymbol{\omega}^T \mathbf{x} + b \cdot$$

The neuron can also be equipped with a transfer function, also called an activation function, see Fig. 1. We will denote this function as $\sigma : \mathbb{R} \to \mathbb{R}$. It transforms the weighted sum s into an activation $z = \sigma(s)$. Therefore, the expression of the "complete" artificial neuron is:

$$y = \sigma\left(\boldsymbol{\omega}^T \mathbf{x} + b\right) \cdot$$

This equation represents a neuron that takes multiple inputs, applies a weight to each, sums them up, adds a bias, and then passes the result through an activation function to produce the final output. The activation function introduces non-linearity into the model, allowing the neural network to learn and represent more complex patterns. There are many different activation functions that can be used in artificial neurons, each with its own properties and use cases. The choice of activation function can significantly impact the model performance. Here are a few examples:

- **Linear Function**: The linear function adjusts the input's magnitude and does not affect whether the input is positive or negative.
- **Sigmoid Function**: The sigmoid function is a type of squashing function that transforms the input into a range between 0 and 1. This is particularly useful for models that need to predict probabilities as outputs.
- **Hyperbolic Tangent Function**: The hyperbolic tangent function is also a squashing function. It transforms the input to a range between -1 and 1. Being zero-centered, it helps the model learn patterns in the data more effectively.
- **Rectified Linear Unit Function**: The rectified linear unit (ReLU) function is currently the most widely used activation function in neural network-based models. It outputs x if (x) is positive, and 0 otherwise.

https://doi.org/10.5194/wes-2024-189
Preprint. Discussion started: 15 January 2025

eawe european academy of wind energy
Open Access WIND ENERGY SCIENCE DISCUSSIONS

– **Exponential Linear Unit Function**: The exponential linear unit is a variant of the ReLU function. It addresses the vanishing gradient problem by assigning negative values when $x < 0$.

– **Softmax Function**: The softmax function is often used in the final layer of a neural network-based classifier. It represents a probability distribution over different possible outcomes.

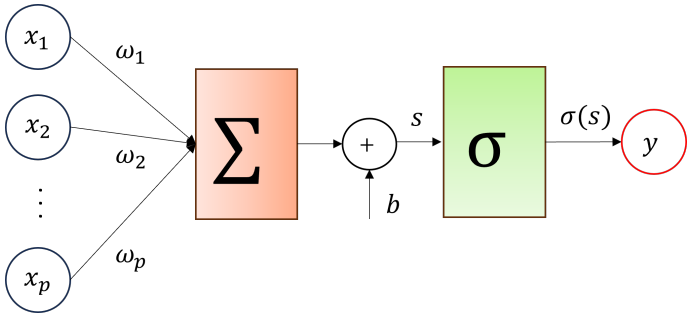

Figure 1. Graphical representation of a formal neuron. The neuron performs the weighted sum of the input activations, plus a bias. This quantity then passes through a an activation function Φ.

Previously, we have presented the concept of shallow network where only one hidden layer was considered. However, increasing the number of hidden layers in a neural network can enhance the model's ability to capture complex patterns and relationships in the data. This is because each layer in the network can learn to represent different levels of abstraction. Nevertheless, it is important to note that adding more layers also increases the risk of overfitting, where the model learns the training data too well and performs poorly on unseen data. Therefore, the decision to increase the number of hidden layers should be made carefully, considering the complexity of the task and the amount of available data.

In that context, a feed-forward artificial neural network (FNN) is a set of formal neuron previously described which are organized in layers (Goodfellow et al., 2016). The autoencoder used in this paper relies on this specific feed-forward network architecture allowing to learn the most important features of the input. Mathematically, the p-dimensional input parameter vector, denoted by $\mathbf{x}$, is passed forward through H hidden layers of neurons in order to compute the output vector y. Each hidden layer consist of hidden neurons at which the incoming information is processed by the two steps previously described. Firstly, at each hidden neuron j from the first hidden layer the output $s^{(1)}$ is calculated by linearly scaling the input as follows:

$$s^{(1)} = \sum_{i=1}^{p} \omega_{ij}^{(1)} x_i + b_j^{(1)},$$

where x_i is the i-th element of the input vector, $\omega_{ij}^{(1)}$ the weight connection between x_i and the j-th hidden neuron from the first layer, and $b_j^{(1)}$ the bias offset for the j-th neuron. Secondly, the result is passed through an activation function σ:

$$y^{(1)} = \sigma(s^{(1)}).$$

https://doi.org/10.5194/wes-2024-189
Preprint. Discussion started: 15 January 2025

eawe european academy of wind energy
Open Access WIND ENERGY SCIENCE DISCUSSIONS

The activated output then serves as input to the next layer, such that with the predefined total number of hidden layers. By considering $\mathbf{X}$ as a random variable with values in $\mathbb{R}^p$ having a number of H hidden neurons with a corresponding nonlinear activation function σ_h, we can define the complete FNN with the function $f_H : \mathbb{R}^p \to \mathbb{R}^{p_H}$ defined as:

$$f_H : \begin{cases} f_0(\mathbf{x}) = \mathbf{x} \\ f_h(\mathbf{x}) = \sigma_h(\mathbf{W}_h f_{h-1}(\mathbf{x}) + b_h), \quad \forall h \in [1, \ldots, H] \end{cases},$$

where, $\mathbf{W}_h \in \mathbb{R}^{p_h \times p_{h-1}}$ is the matrix containing the weights between layer $h-1$ and the layer h and b_h is the added bias to the layer h. In the training phase of an ANN, the goal is to estimate the weight parameters, denoted as $\mathbf{W}$, and bias parameters in such a way that the loss function result, i.e., the difference between the estimated output and the observed output, is minimized. This process can be achieved through the use of various optimization algorithms that iteratively find the parameters which minimize a selected loss function. The training process involves a technique known as back-propagation, which consists of two steps. The first step involves calculating the derivative of the loss function with respect to the weights. These derivatives are then utilized in the second step to update the model parameters. The term "epochs" refers to the number of iterations required to reach predefined stopping criteria. To evaluate the performance of the model, cross-validation (CV) can be used. This method estimates the generalization error by using different splits of training and testing data. It is evident that there are several hyper-parameters that need to be chosen in relation to the network structure (such as the number of layers and the number of neurons in each layer) and the training process (for example, weight initialization, learning rate, regularization factor, optimizer, etc.). The autoencoder, as illustrated in Fig. 2, is composed of two interconnected FNNs. The first network, known as the encoder, reduces the data's dimensionality. The second network, referred to as the decoder, restores the data to its original dimension. The encoder and decoder have an equal number of layers and neurons, but their order is reversed. One of the strengths of autoencoder architectures lies in their adaptability to specific use cases. This adaptability is highlighted in (Berahmand et al., 2024), which provides detailed insights into how autoencoders can be customized for various applications. By considering $\mathbf{X}$ as a random variable with values in $\mathbb{R}^p$, an ANN, such as an autoencoder, models a function $\mathcal{H}$ such that:

$$|| \mathcal{H}(\mathbf{x}) - \mathbf{x}|| \leq \epsilon.$$

Mathematically, it means that the image of $\mathbf{x}$ is a reconstruction of $\mathbf{x}$ with an error of ϵ. As said previously, to perform this reconstruction the autoencoder is decomposed into two parts:

- an encoder, i.e., a function $\mathcal{E} : \mathbb{R}^p \to \mathbb{R}^d$,
- a decoder, i.e., a function $\mathcal{D} : \mathbb{R}^d \to \mathbb{R}^p$.

By using this formalism, $\mathcal{H}$ is the successive application of encoding and then decoding, such that:

$$\mathcal{H} = \mathcal{D} \circ \mathcal{E}.$$

In principle, the encoder compresses the information by reducing the dimension of $\mathbf{x}$. So generally, the principle is to encode $\mathbf{x}$ with fewer variables than the input vector, such that $d \leq p$. Subsequently, we denote $\mathbf{z} = \mathcal{E}(\mathbf{x})$ as the vector of latent variables

https://doi.org/10.5194/wes-2024-189
Preprint. Discussion started: 15 January 2025

eawe european academy of wind energy
Open Access WIND ENERGY SCIENCE DISCUSSIONS

associated with $\mathbf{x}$. The objective of the training phase is to seek the weights and biases such that:

$$(\mathbf{W}, \mathbf{b})^* = \text{argmin}_{(\mathbf{W},\mathbf{b})} \mathcal{L}(\mathbf{x}, \overline{\mathbf{x}}),$$

where $\mathcal{L}$ is a regression cost function, e.g., mean squared error or mean absolute error.

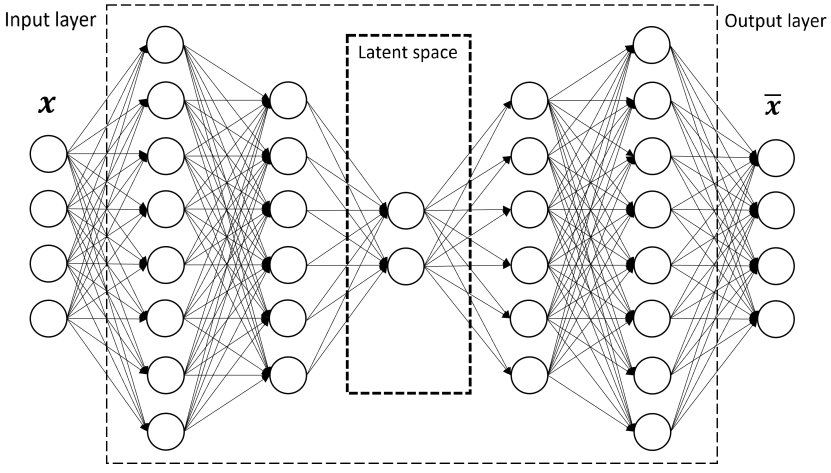

Figure 2. Graphical representation of an example autoencoder.

As said previously, the encoder compresses $\mathbf{x}$ by reducing its dimensionality while the decoder reconstructs $\mathbf{x}$ from the latent space $\mathbf{z}$. The space in which $\mathbf{z}$ evolves aims to be an underlying space that effectively explains the structure of the data $\mathbf{x}$. The concept is that significant differences in the observation space can be explained by small variations in the latent space due to underlying regularities in the distribution. This type of deep-learning architecture can be employed for anomaly detection by training the autoencoder with data from normal operating conditions. This training process allows to learn a mapping function that successfully reconstructs normal data samples with a very small reconstruction error. Then, the neural network is adept at reconstructing regular data, but struggles when presented with data from irregular operating conditions. Finally, anomalies can be identified by examining the discrepancy between the input data and the reconstructed data.

After fitting the autoencoder model, the next step involves determining an appropriate threshold for distinguishing between normal and anomalous sequences. One common approach is to set the threshold based on a quantile of the reconstruction error distribution. If the quantile is set to be high, more anomalous sequences will be classified as normal; conversely, a lower quantile will result in normal patterns being labeled as anomalous. As depicted in Fig. 3, the choice of the threshold depends significantly on the specific study case. Based on the arbitrary value obtained from the training set, the future examples can be classified as anomalous if the reconstruction error is higher. In the presented study, we have set the threshold at $\mu + 3 * \sigma$ where μ and σ are respectively the mean and the standard deviation for the training reconstruction error.

Previously, we focused on neural structures of the type known as FNNs. Nevertheless, these models have considerable practical limitations. Indeed, the use of fully connected layers is not suitable for all types of observations. In fact, the number of parameters in a multilayer perceptron grows rapidly with the dimension of the input and the dimension of the hidden

https://doi.org/10.5194/wes-2024-189
Preprint. Discussion started: 15 January 2025

eawe european academy of wind energy
Open Access WIND ENERGY SCIENCE DISCUSSIONS

layer. This explosion in the number of parameters poses two problems. First, computational costs increase, both in terms of computation time and the memory required to store the model's weights. Second, the massive increase in the number of parameters promotes overfitting and thus complicates decision modeling. In our research, we suggest utilizing convolutional autoencoders to identify and extract the most significant features from the input data. Such convolutional autoencoders leverage convolutional layers for feature extraction and an encoder-decoder architecture to learn compact representations of input data.

In this context, it is necessary to rely on the architecture of convolutional neural networks (CNNs) that allows for an a priori understanding of the spatial structure of the data. The fundamental operation in a CNN is the convolution operation between two function $f : \mathbb{R} \to \mathbb{R}$ and $g : \mathbb{R} \to \mathbb{R}$, defined as:

$$(f * g)(x) = \int_{-\infty}^{+\infty} f(t)g(x-t)dt\cdot$$

Even though the equation above is valid for univariate functions, it extends without difficulty to functions of several variables. In this case, the integral then covers the set of variables, i.e., multiple integral. Then, convolutional autoencoders (CAEs) are a specialized type of autoencoder that leverage layers with such convolutional operation (Lee and Carlberg, 2020). In the realm of signal processing, these convolutional autoencoders have been used to extract signal features (Wu et al., 2022). In summary, the ability of convolutional autoencoders to combine the strengths of autoencoders and convolutional neural networks makes them valuable tools for various signal processing tasks.

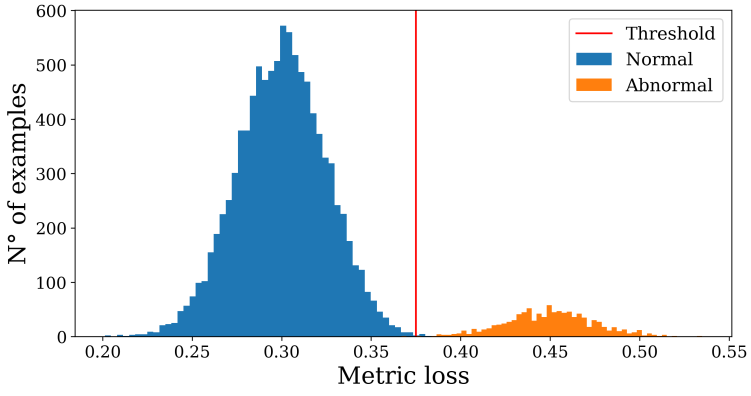

Figure 3. Representation of the losses distribution of an autoencoder for the non-anomalous detection.

3 A study case: the Zefyros floating offshore wind turbine

3.1 Study description and data preparation

Unitech Zefyros is a floating spar offshore wind turbine originally installed as Hywind Demo by Equinor (Statoil) at approximately 11 kilometres of the west cost of Karmøy (Norway) (Ibrion and Nejad, 2023). The floater configuration is based on

https://doi.org/10.5194/wes-2024-189
Preprint. Discussion started: 15 January 2025

a cylinder-shaped structure which is submerged vertically, see Fig. 4. This offshore floating system is supporting a Siemens 2.3-MW wind turbine with a rotor diameter of 82.4 meters. Table 1 contains key data for the SWT-2.3-82 wind turbine and the floating platform structure. Due to the long distance between the center of gravity and center of buoyancy, the structure stability has shown promising behavior. Indeed, the floating platform is known for its deep draft which gives the buoy very stable and good hydrodynamic characteristics. The spar limits wave-induced movements and loading to the structure by reducing the cross-sectional area in the splash zone, while at the same time reducing the substructure cost.

The Hywind Demo structure involves a unique design where the wind turbine was supported by an underwater floating structure, similar to those used in offshore oil rigs (Liu et al., 2019). The Zefyros platform is ballast stabilized and moored to the seabed by a system of three separate catenary mooring lines. At the sea floor, these mooring lines are fixed to drag anchors. Near the still-water sea level, the mooring line is split into a bridle attachment that connects to the hull. This mooring configuration allows to increase the system yaw stiffness. Moreover, large clump weights are attached to each mooring line close to the mid-span of the line. The design of the mooring lines incorporates also chain and wire to achieve the desired force-displacement characteristics. The success of the FOWT system is evident from its flawless operation over the years, demonstrating its ability to withstand various wind and wave conditions (Jacobsen and Godvik, 2020).

Figure 4. The Zefyros floating offshore wind turbine relies on a Siemens 2.3-MW. Credits: Unitech Energy Group

https://doi.org/10.5194/wes-2024-189
Preprint. Discussion started: 15 January 2025

eawe european academy of wind energy
Open Access WIND ENERGY SCIENCE DISCUSSIONS

Zefyros's impact extends beyond its individual structure, as its design and the conception methodologies have influenced the design of the new structures for offshore wind turbines, contributing to the economic viability of offshore wind energy generation in deep waters Ibrion and Nejad (2023). Indeed, the first floating wind turbine's measurements and simulations have provided valuable insights into the performance and behavior of floating wind turbines, guiding further research and development in this promising technology field (Skaare et al., 2014).

Property	Value
Depth to Platform Base Below SWL (m)	100.045
Elevation to Platform Top (Tower Base) Above SWL (m)	17.000
Platform Mass (kg)	4,855,290.000
CM Location Below SWL along Platform centerline (m)	-74.770
Hub Height (m)	65
Hub Mass (kg)	26,400
Rotor Diameter (m)	82.4

Table 1. Zefyros Properties - (SWL: still water level)

Hereafter, two strategies for identifying operating phases of this wind turbine system using high-frequency sensor data have been developed. The first strategy is based on an engineering signal processing approach. The underlined methodology relies on the kurtosis analysis of a time signal related to the magnetometer located close to the rotor-nacelle-assembly. One major advantage is that magnetometers are sensitive to electromagnetic interference from sources other than the Earth's magnetic field. In our context, permanent magnet generators are used in the wind turbine system generating a time-varying magnetic field. Such variation can be detected using a magnetometer, which measures the strength and direction of magnetic fields. In summary, by analyzing the acquired magnetic data from a magnetometer placed near the wind turbine generator, one can detect changes in the magnetic field patterns, which can provide valuable insights into the operational status of the generator.

The second strategy, which is based on an autoencoder mathematical approach, has the capability to facilitate the detection of deviations from a standard behaviour established in a reference dataset. If necessary, the neural network architecture can identify the frequency range of the anomaly by examining the reconstruction error per frequency band. Indeed, in our study case, the neural network takes the power spectrum density of sensor channels as input. The autoencoder process will then recognize common patterns in the spectrum. If these common patterns are not provided as input to the network, the model will struggle to reconstruct the power spectrum density (PSD). As previously mentioned, the in-situ data used to train and test the autoencoder in this study were based on the measurements obtained from the tri-axial accelerometers with an acquisition rate of 40 hertz and located inside the mast of the floating wind turbine, as illustrated in Fig. 5. Their response in the frequency-domain using the PSD has been studied for each one-hour acceleration response of the system. Besides the advantage of not

https://doi.org/10.5194/wes-2024-189
Preprint. Discussion started: 15 January 2025

eawe european academy of wind energy
Open Access WIND ENERGY SCIENCE DISCUSSIONS

using the heavy time series, the spectral response contains information on different physical phenomena as illustrated in Fig. 6, which can be identified thanks to techniques such operational modal analysis (Brincker and Ventura, 2015; Reynders, 2012).

Figure 5. S-Morpho Installation in the Tower.

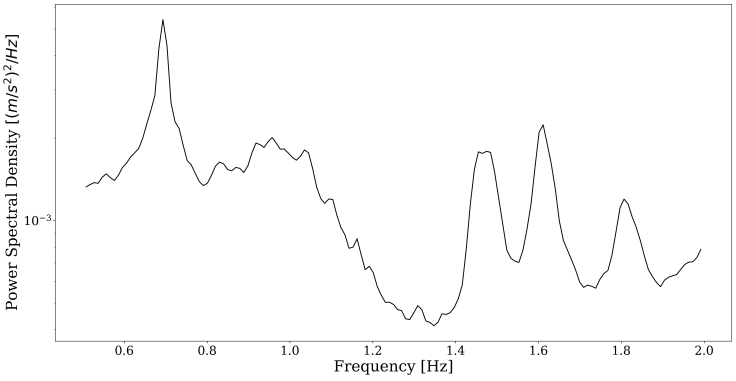

Figure 6. Power spectral density of the tower acceleration measured by S-Morpho sensor obtained through the Welch method.

Due to some limitations in environmental condition measurements and system responses, challenges were encountered in identifying wind turbine anomalies. To address this, the data from tri-axial accelerometer sensors previously described were used to identify operating state of the system. However, the acceleration data alone do not directly reveal the turbine's operating state. Additionally, during the project, we had access to a limited number of SCADA variables, see Fig. 7, which were averaged over 10-minute intervals for one month. The variables include wind speed at the nacelle, measured by a sonic anemometer, yaw angle, and rotor speed.

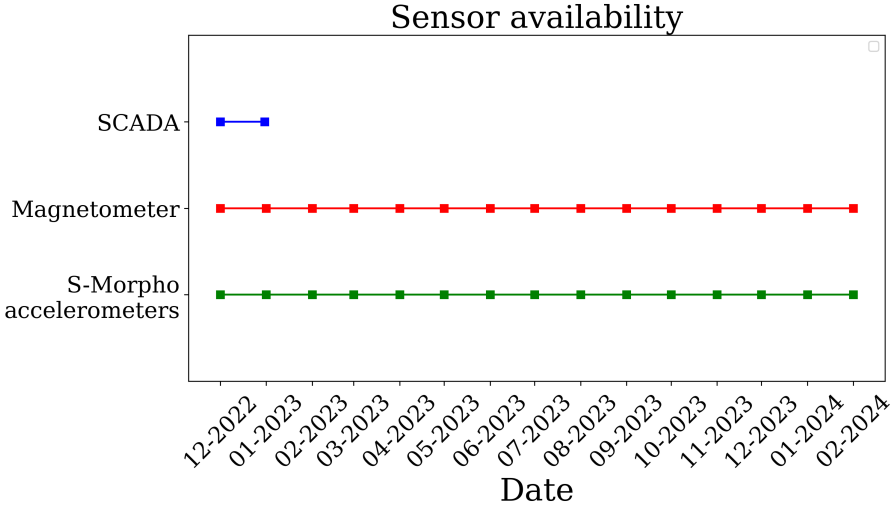

Figure 7. Sensors avalaibility during the measurement campaign.

https://doi.org/10.5194/wes-2024-189
Preprint. Discussion started: 15 January 2025

eawe european academy of wind energy
Open Access WIND ENERGY SCIENCE DISCUSSIONS

These variables from the SCADA system was used to identify the hour period of the wind turbine's operating and non-operating phases. Subsequently, a one-hour averaging and filtering process was applied to the raw data. In particular, the filtering method relies on the different regimes of a wind turbine system. We have focused on the operating regimes of the system. When the wind speed is higher than the cut-in value, the turbine starts to rotate and the generator produces electricity. Then, at the rated wind speed, the turbine reaches its nominal production power according to the converter capacities. Once the rated power is reached, it must be regulated to avoid exceeding the generator's capacity.

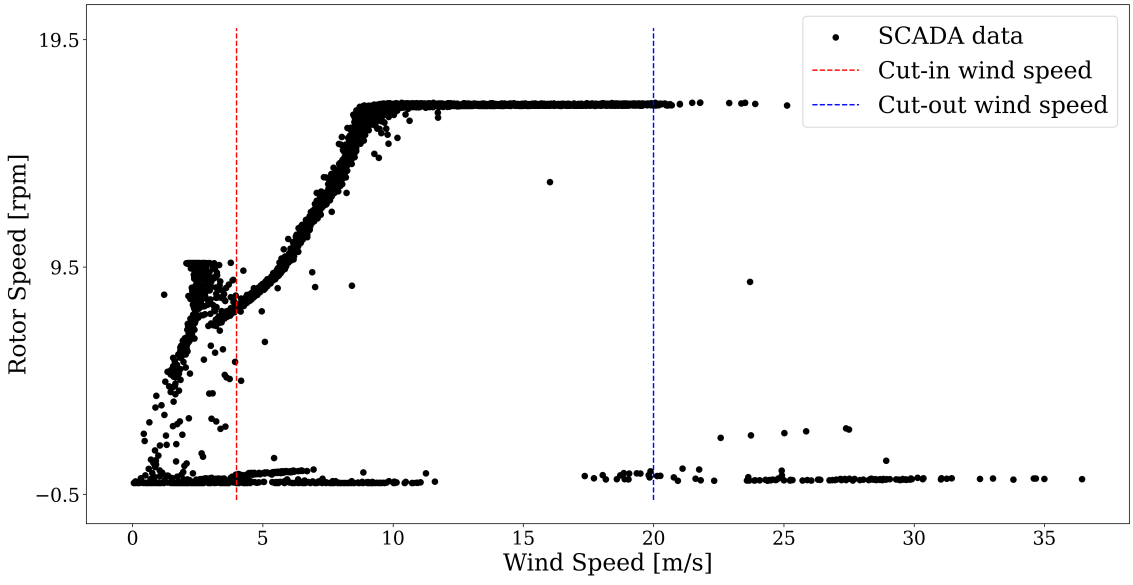

Figure 8. Averaged rotor speed vs. Averaged wind speed data over 10-minutes from SCADA system.

3.2 Application and results

3.2.1 Signal processing approach

The analyzed magnetic signal has been acquired by the 3-axis measurement system S-Morpho, which includes three accelerometers, three magnetometers, and one temperature sensor. As mentioned previously, only one sensor node has been selected for this analysis campaign, i.e., the closest sensor to the RNA. For more details on the location and orientation of the sensor nodes installed on the wind turbine tower, see (C. and M., 2024). A spectral analysis of the magnetic timeseries was carried out as pre-processing step in order to determine and visualize the frequency band of the rotating machinery inside the RNA. As shown in the spectogram in Fig. 9, a dominant frequency emerged at around 11 Hz when the system operated at its rated condition. This frequency may be related to the high-speed shaft rotation inside the generator. The rotation of the low-speed shaft (rotor) is illustrated by the black line at the bottom in Fig. 9, in revolutions per minute. This bottom image of Fig. 9 also depicts the temporal series of the magnetic signal as the blue line. A significant change in magnitude can be seen around the 4500-seconds

https://doi.org/10.5194/wes-2024-189
Preprint. Discussion started: 15 January 2025

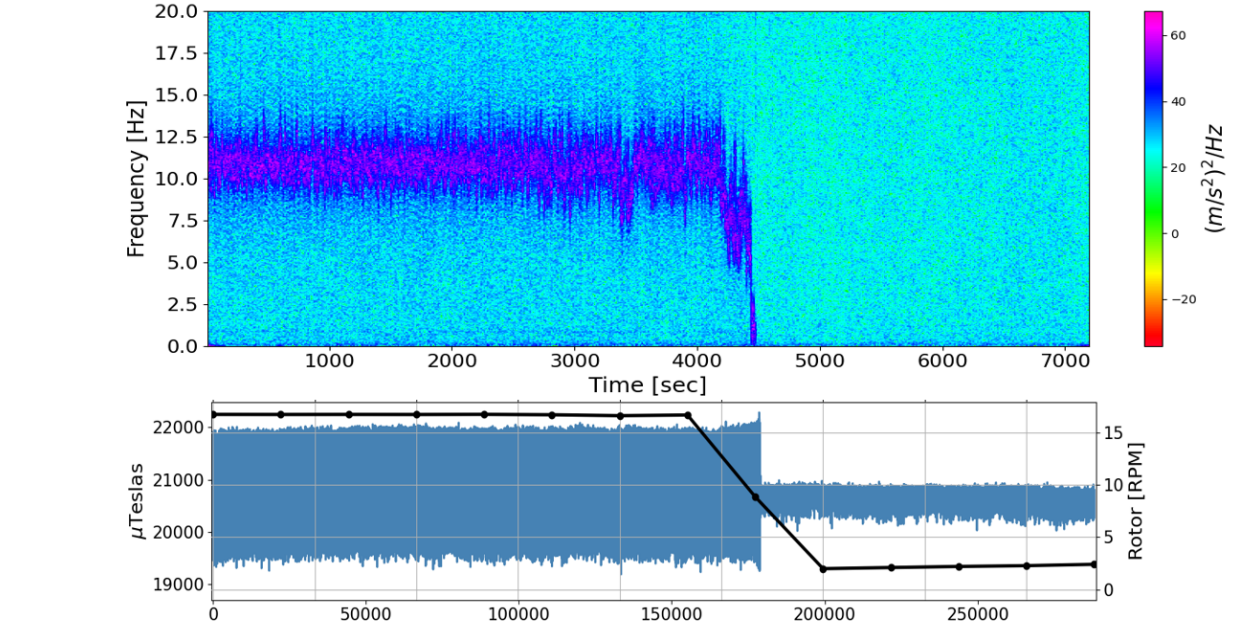

Figure 9. The magnetic signal spectrogram of the closest sensor to the RNA along y-axis (upper figure). Magnetic time series and rotor rotation from collected SCADA data in blue and black lines respectively (lower figure))

It is important to note how the signal is affected by the rotation machinery, as seen in the spectogram after 4500-second. During this period, the signal seems to approach a Gaussian noise when the low-speed shaft comes to a complete stop. With no energy production and no rotation, there is no magnetic interference detectable by the magnetometer sensor. Given this context, kurtosis analysis is an appropriate indicator, as it describes the characteristics of the dataset in terms of the distribution's tails based on a Gaussian distribution.

In that context, a detection methodology was develop in order to identify the magnetic signal changes in function of the wind turbine operating state and the statistical indicator. Firstly, a specific period of the magnetic signal was selected to compute the kurtosis indicator based on a one-hour time window. The kurtosis values were then compared to the SCADA values in order to determine the thresholds used later for the detection criteria and binary classification.

During the comparison, two operating states were identified: the first when the turbine operates at rated capacity (around 16 RPM) and the second under-rated condition (rotations below 16 RPM). These variations in rotation affect kurtosis estimation, causing the indicator values to fall between the three kurtosis categories: mesokurtic, platykurtic, and leptokurtic. This effect can be seen during the first days of the studied month, as shown in Fig. 10. Thus, two kurtosis thresholds were defined, a lower at 2.8 and a higher at 4. Once the thresholds were defined, the magnetic temporal signal of December 2022 was analysed based

https://doi.org/10.5194/wes-2024-189
Preprint. Discussion started: 15 January 2025

eawe european academy of wind energy
Open Access WIND ENERGY SCIENCE DISCUSSIONS

on different time windows for the kurtosis estimation. In Fig. 10, the kurtosis values of December 2022 are depicted as the orange line for one-hour time window.

Then, the magnetic signal was classified in function of the thresholds as follows:

- If kurtosis $>$ 4 wind turbine operating state.
- If 2.8 $<=$ kurtosis $<=$ 4 wind turbine non-operating state (default detection)
- If kurtosis $<$ 2.8 wind turbine operating state

The two black dashed lines, in Fig. 10, correspond to the selected threshold values, at 2.8 and 4.

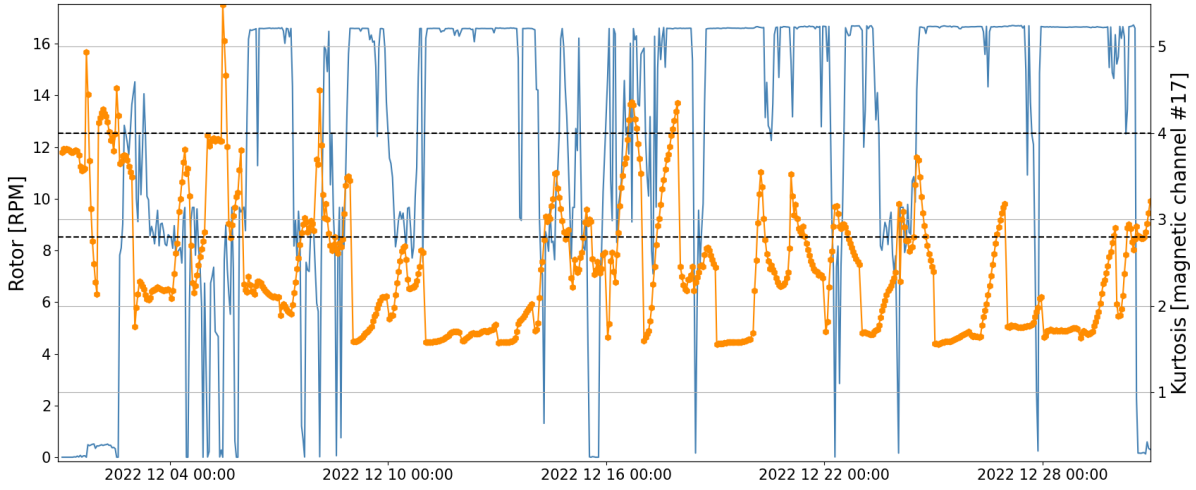

Figure 10. Temporal signal of SCADA rotor angular velocity as the blue line, and kurtosis estimation in orange. The two defined kurtosis thresholds are depicted as the two dashed lines.

3.2.2 Convolutional autoencoder approach

The accelerometers allow to measure the vibration response of the wind turbine tower. These measurements were obtained under varying environmental conditions, including different wind and wave intensities and directions. Given this context, the measurements are particularly sensitive to excitation properties. To ensure accurate anomaly detection, we trained a convolutional autoencoder using input samples that adequately cover the environmental condition space. If the autoencoder is not exposed to a diverse range of environmental conditions during training, it may incorrectly reconstruct the PSD response due to unseen excitations. One of the significant challenges we faced was defining the validity domain of the model, which relies on the environmental conditions present in the training dataset. An environment is considered within the model's validity domain if it does not deviate significantly from at least one environment encountered during training. To achieve this, we leveraged environmental conditions from weather numerical prediction models. Subsequently, we identified distinct training and testing

https://doi.org/10.5194/wes-2024-189
Preprint. Discussion started: 15 January 2025

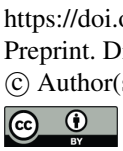

eawe european academy of wind energy
Open Access WIND ENERGY SCIENCE DISCUSSIONS

sets by fitting a multi-dimensional histogram and carefully selecting different one-hour periods for each wind turbine status. As depicted in Fig. 11, we thoroughly explored the entire environmental conditions space in both the training and testing datasets. By following this process, the autoencoder was trained on approximately 86% of the data and tested on the remaining 14% to prevent overfitting.

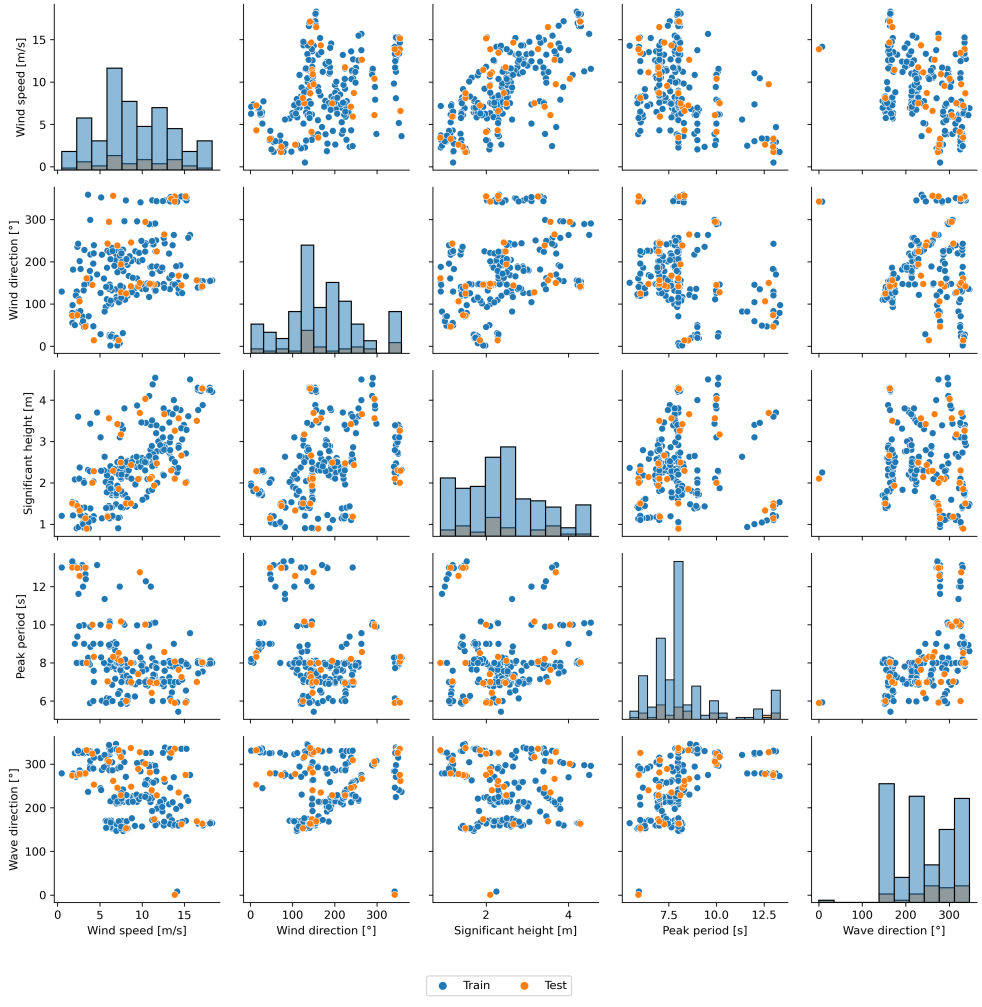

Figure 11. Stratified environmental input space on operating phase of the Zefyros floating offshore wind turbine to split the input data into train (blue dots) and test sets (orange dots).

As illustrated in the Fig. 12, two distinct sets of accelerations can be identified based on the wind turbine system's one-hour operating conditions. Ultimately, 257 operating hour periods with their associated accelerations along the tower were identified in the raw data. Conversely, 24 non-operating statuses of the wind turbine were highlighted using the rotor speed from the SCADA system.

https://doi.org/10.5194/wes-2024-189
Preprint. Discussion started: 15 January 2025

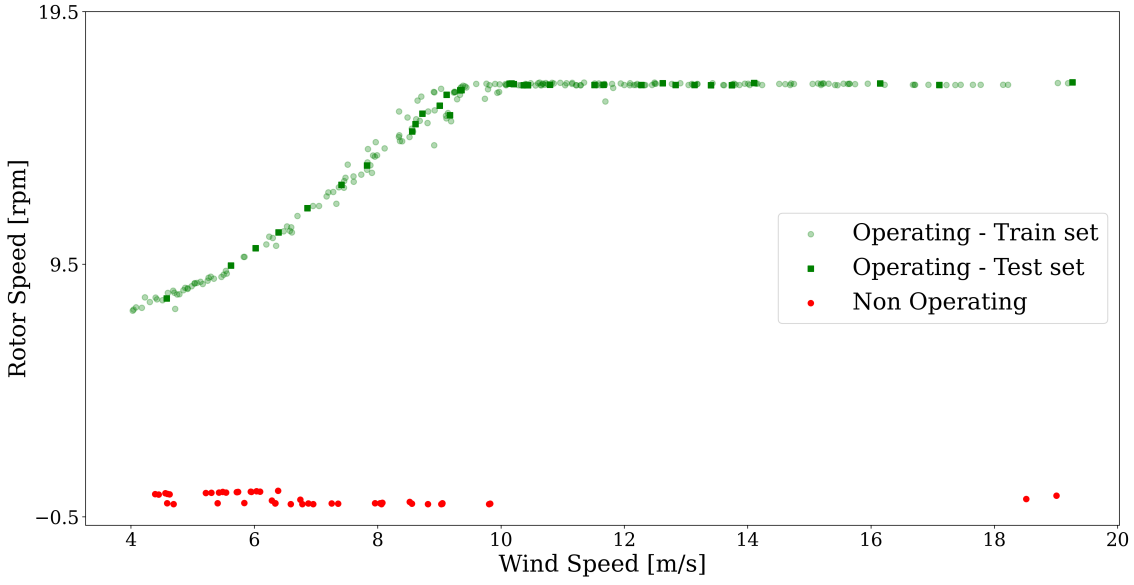

Figure 12. Rotor vs. wind speeds data from limited-SCADA with operating and non-operating 1-hour period.

The autoencoder under consideration is outlined in Tab. 2. A ReLU activation function is employed between each layer, with the exception of the final layer, which uses a sigmoid function. During the training phase, the ANN architecture underwent parameter optimization using the Adam optimization algorithm, with a learning rate of 0.001 and a batch size of 5. The model was trained using back-propagation, with mean squared error serving as the loss function and defined as:

$$\mathcal{L}(\mathbf{x},\overline{\mathbf{x}}) = \frac{1}{n_{signal}} \sum_{i=1}^{n_{signal}} (x_i - \overline{x}_i)^2,$$

where, n_{signal} is the frequencies number in the PSD. Then, to detect when the wind turbine is operating, the reconstruction loss produced from the autoencoder can be used to find out how well the signals are reproduced. Since the architecture has been trained on accelerations from operating periods, the model has learned the relations between the signals for such conditions. If the residual is larger for new data than a threshold obtained from the training error, see Fig. 13, there is potentially non-operating status for the system.

https://doi.org/10.5194/wes-2024-189
Preprint. Discussion started: 15 January 2025

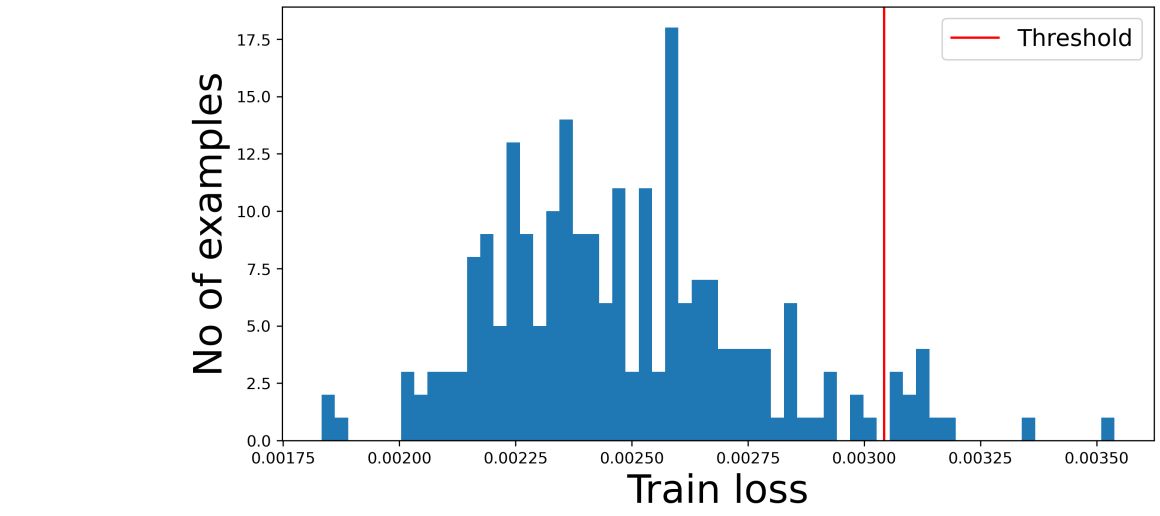

Figure 13. Representation of reconstruction error distribution applied to the training set on acceleration dataset from operating periods.

Model	Architecture
Convolutional autoencoder	Input: $1 \times 18 \times 615$ (channels $\times$ height $\times$ width) Encoder: - Layer 1: 2D-Convolutional Layer (16, (2, 3), 2, 1) ReLu activation function Dropout layer with 0.1 rate - Layer 2: 2D-Convolutional Layer (32, (4, 3), 2, 1) ReLu activation function Dropout layer with 0.1 rate Decoder: - Layer 1: Transpose 2D-Convolutional Layer (32, (4, 3), 2, 1) ReLu activation function - Layer 2: Transpose 2D-Convolutional Layer (16, (2, 3), 2, 3) Sigmoid activation function

Table 2. Architecture of the convolutional autoencoder with each convolutional layer defined as (number of channels produced, size of the kernel, stride of the convolution, padding added) and transposed convolutional layer defined as (number of channels produced, size of the kernel, stride of the convolution, padding added).

https://doi.org/10.5194/wes-2024-189
Preprint. Discussion started: 15 January 2025

eawe european academy of wind energy
Open Access WIND ENERGY SCIENCE DISCUSSIONS

3.2.3 Results

The detection ability of the procedures has been tested on two distinct test sets, i.e., one dataset with identified operating period and the other one with non-operating behavior. In the process of evaluating the performance of the anomaly detection procedure, key metrics such as precision and recall are usually computed. Precision, in the context of a binary classifier, quantifies the likelihood that a detected anomaly is indeed a true anomaly. The mathematical definition of precision is as follows:

$$\text{Precision} = \frac{\#TruePositives}{\#TruePositives + \#FalsePositives}.$$

On the other hand, the recall metric, often referred to as sensitivity, estimates the system's proficiency in identifying anomalies. The formal definition of recall is as follows:

$$\text{Recall} = \frac{\#TruePositives}{\#TruePositives + \#FalseNegatives}.$$

The calculated performance metrics for precision and recall on both detection test sets are summarized in Tab. 3. The proposed non-operating detection method, based on a convolutional ANN demonstrates sufficient sensitivity in identifying wind turbine operating phases using tower accelerometer measurements. Notably, we achieved this without relying on feature engineering; instead, we allowed the autoencoder to learn spectral density patterns during the wind turbine's operational periods.
In Tab. 3, it can also be seen that the signal processing approach has lower performance than the convolutional ANN model. As an statistical method, kurtosis value of a given distribution changes in function of the sample size. When the sample is small, kurtosis values are highly variable. Therefore, the use of a large time window for kurtosis may have significant impacts on the detection method.

Table 3. Detection performance of the kurtosis analysis and the anomaly detection method based on a convolutional ANN on a test dataset.

	Kurtosis procedure		Convolutional ANN	
	Operating	Not-Operating	Operating	Not-Operating
Recall	0.939	0.750	0.970	0.917
Precision	1.000	1.000	1.000	1.000

In order to test the time window effect, an analysis based on a 10 min time window was performed. Here, the data of the full month was used, i.e., without the filtering explain above. The performance of this method was again compared to the SCADA data sampled at 10 min. From Tab. 4, it can be seen that the performance has diminished. This difference is mainly due to the augmented size of the data-set.

https://doi.org/10.5194/wes-2024-189
Preprint. Discussion started: 15 January 2025

eawe european academy of wind energy
Open Access WIND ENERGY SCIENCE DISCUSSIONS

Table 4. Detection performance of the 10 min time window of kurtosis method.

Test set	Precision	Recall
Operating	0.99	0.887

4 Conclusions

Floating offshore wind energy is experiencing robust growth not only in Europe but globally. A significant portion of the levelized cost of energy is attributed to the operation and maintenance costs of such complex structures. The use of condition monitoring and artificial intelligence offers potent solutions for the automated early detection of abnormal wind turbine behaviour under varying operational conditions.

The research work presented in this paper aimed to detail two condition monitoring procedures to detect unwanted downtime periods. The first method leverages the analysis of signals derived from magnetometers to identify anomalies. Magnetometers measure the geomagnetic field, which typically exhibits stable patterns under normal operating conditions. By continuously acquiring and preprocessing these signals, we can monitor the possible variations in the field. The principle of this method involves calculating the statistical metric of kurtosis. This mathematical solution quantifies the shape of the data distribution, particularly focusing on the tails relative to the peak, which aids in identifying outliers or unusual patterns. Under normal conditions, the kurtosis of the magnetometer signals remains within a certain range, but deviations from this range indicate potential unwanted behaviour. By setting thresholds, the approach can flag significant variations in kurtosis, thus detecting anomalies related to unwanted downtime in our context. This approach provides a robust mechanism for real-time anomaly detection and can be integrated into the wind turbine's monitoring systems to enhance operational reliability and maintenance efficiency when SCADA is not available.Then, the proposed deep-learning approach for detecting unwanted downtime periods in wind turbines employs autoencoders, a specialized type of neural network architecture, to produce outputs identical to their inputs. These models are trained in an unsupervised manner to learn optimal representations of operational scenarios. The novelty of this method lies in the use of a 2D-convolutional autoencoder, which is coupled with power spectra derived from on-site tower accelerations of the floating structure. These spectra, similar to magnetic fields, are extracted from time series data spanning one hour and encompass a wide range of metocean and wind conditions. The autoencoder is trained using this input data, with the network's training dataset comprising operational data obtained through an analysis of SCADA variables. This deep neural network architecture can accurately reconstruct inputs with similar characteristics, enabling the detection of anomalies by identifying discrepancies between the input and reconstructed output, which may to potential downtime periods. The proposed methodology enables the autoencoder to autonomously learn and extract spectral features tailored to the components being monitored, eliminating the need for human intervention.

Both detection methodology was validated using in-situ data collected from high-frequency sensors installed on the Zefyros floating offshore wind turbine. In conclusion, the deep-learning approach utilizing a 2D-convolutional autoencoder demonstrates superior performance in detecting unwanted downtime periods of wind turbines compared to the kurtosis signal analysis method. This comparison is substantiated by the recall results obtained from both procedures, which highlight the enhanced

https://doi.org/10.5194/wes-2024-189
Preprint. Discussion started: 15 January 2025

accuracy of the convolutional autoencoder, particularly in identifying non-operational periods of the offshore floating wind turbine. The autoencoder's ability to learn complex patterns from power spectra derived from tower accelerations under various metocean and wind conditions enables more precise anomaly detection. Consequently, this advanced deep-learning technique proves to be more effective and reliable, offering significant improvements over traditional kurtosis-based signal analysis for monitoring and maintaining wind turbine operations. The results obtained are highly encouraging, demonstrating the method's ability to successfully differentiate between operational and non-operational periods.

While the current study provides a promising start, there is scope for further investigations to enhance the condition monitoring procedure. Further studies are needed for applications beyond the operational statuses detection of the floating offshore wind turbine. The major challenge of the presented study was the limited access to SCADA data over a one-month period. Therefore, to detect and diagnose anomalies more effectively, it is necessary to gather more comprehensive information from the physical asset. Indeed, in the context of FOWT systems, it is valuable to explore and assess the developed damage detection methods across various damage types and intensities. Leveraging aero-servo-hydro-elastic simulations, we can investigate the system's response to different damage scenarios. Additionally, considering the temporal aspect is crucial when devising an effective anomaly detection strategy. As damage accumulates over time, understanding the progressive influence on detection accuracy becomes essential.

Code availability. The code used in this study is available upon request. Researchers and interested parties can obtain access by contacting the corresponding author. This approach ensures that the code is shared responsibly and that any questions regarding its use can be addressed directly. We are committed to promoting transparency and reproducibility in research, and we encourage collaboration and further exploration of our work.

Author contributions. This study on comparative anomaly detection for floating offshore wind turbines using in-situ data was a collaborative effort among all authors. Each author made significant contributions to the research and preparation of the manuscript. Adrien Hirvoas conceptualized the study, designed the methodology, and supervised the project. He also played a key role in data analysis, interpretation, and writing of the manuscript. Cesar Aguilera, Matthieu Perrault, and Damien Desbordes provided expertise in post-treatment of the in-situ data obtained from the accelerometers. They also reviewed and edited the manuscript for technical accuracy and clarity. Romain Ribault provided expertise in offshore wind turbine technology and in-situ data acquisition. He also reviewed and edited the manuscript for technical accuracy and clarity.

Competing interests. The authors declare that they have no known competing financial interests or personal relationships that could have appeared to influence the work reported in this paper.

https://doi.org/10.5194/wes-2024-189
Preprint. Discussion started: 15 January 2025

eawe european academy of wind energy
Open Access WIND ENERGY SCIENCE DISCUSSIONS

References

Bangalore, P. and Tjernberg, L. B.: An artificial neural network approach for early fault detection of gearbox bearings, IEEE Transactions on Smart Grid, 6, 980–987, 2015.

Barahona, B., Hoelzl, C., and Chatzi, E.: Applying design knowledge and machine learning to scada data for classification of wind turbine operating regimes, in: 2017 IEEE Symposium Series on Computational Intelligence (SSCI), pp. 1–8, IEEE, 2017.

Berahmand, K., Daneshfar, F., Salehi, E. S., Li, Y., and Xu, Y.: Autoencoders and their applications in machine learning: a survey, Artificial Intelligence Review, 57, 28, 2024.

Brincker, R. and Ventura, C.: Introduction to operational modal analysis, John Wiley & Sons, 2015.

C., A. and M., D.: 20240305 DIONYSOS WP04 Task4.1a Local SHM digital twin on FOWT floater, [Unpublished manuscript], 2024.

Chen, S. and Guo, W.: Auto-encoders in deep learning—a review with new perspectives, Mathematics, 11, 1777, 2023.

Cui, Y., Bangalore, P., and Tjernberg, L. B.: An anomaly detection approach based on machine learning and scada data for condition monitoring of wind turbines, in: 2018 IEEE International Conference on Probabilistic Methods Applied to Power Systems (PMAPS), pp. 1–6, IEEE, 2018.

Dhiman, H. S., Deb, D., Muyeen, S., and Kamwa, I.: Wind turbine gearbox anomaly detection based on adaptive threshold and twin support vector machines, IEEE Transactions on Energy Conversion, 36, 3462–3469, 2021.

Elforjani, M. and Bechhoefer, E.: Analysis of extremely modulated faulty wind turbine data using spectral kurtosis and signal intensity estimator, Renewable Energy, 127, 258–268, https://doi.org/https://doi.org/10.1016/j.renene.2018.04.014, 2018.

Franco, A. M. d. S., Echer, E., Bolzan, M., and Fränz, M.: Study of fluctuations in the Martian magnetosheath using a kurtosis technique: Mars Express observations, Earth and Planetary Physics, 6, 28–41, 2021.

Gonzalez, E., Tautz-Weinert, J., Melero, J., and Watson, S. J.: Statistical evaluation of SCADA data for wind turbine condition monitoring and farm assessment, in: Journal of Physics: Conference Series, vol. 1037, p. 032038, IOP Publishing, 2018.

Goodfellow, I., Bengio, Y., and Courville, A.: Deep learning, MIT press, 2016.

Gorostidi, N., Pardo, D., and Nava, V.: Diagnosis of the health status of mooring systems for floating offshore wind turbines using autoencoders, Ocean Engineering, 287, 115 862, 2023.

Gourvenec, S.: Floating wind farms: how to make them the future of green electricity, accessed 18 July 2022, 2020.

Ibrion, M. and Nejad, A. R.: On a road map for technology qualification, innovation and cost reduction in floating offshore wind: learning from hywind and norwegian approach, Journal of Physics: Conference Series, 2507, 012 008, https://doi.org/10.1088/1742-6596/2507/1/012008, 2023.

Jacobsen, A. and Godvik, M.: Influence of wakes and atmospheric stability on the floater responses of the hywind scotland wind turbines, Wind Energy, 24, 149–161, https://doi.org/10.1002/we.2563, 2020.

Lee, K. and Carlberg, K.: Model reduction of dynamical systems on nonlinear manifolds using deep convolutional autoencoders, Journal of Computational Physics, 404, 108 973, https://doi.org/10.1016/j.jcp.2019.108973, 2020.

Liu, Z., Fan, Y., Wang, W., and Qian, G.: Numerical study of a proposed semi-submersible floating platform with different numbers of offset columns based on the deepcwind prototype for improving the wave-resistance ability, Applied Sciences, 9, 1255, https://doi.org/10.3390/app9061255, 2019.

Nava, V., Ruiz-Minguela, P., Perez-Moran, G., Rodriguez Arias, R., Lopez Mendia, J., and Villate-Martinez, J.-L.: Installation, Operation and Maintenance of Offshore Renewables, Institution of Engineering and Technology, https://doi.org/10.1049/PBPO129E_ch11, 2019.

https://doi.org/10.5194/wes-2024-189
Preprint. Discussion started: 15 January 2025

Ren21, K.: Renewables 2021-Global Status Report: Tech. Rep., 2021.

Reynders, E.: System identification methods for (operational) modal analysis: review and comparison, Archives of Computational Methods in Engineering, 19, 51–124, 2012.

Sae-Ang, B.-I., Kumwilaisak, W., and Kaewtrakulpong, P.: Semi-supervised learning for defect segmentation with autoencoder auxiliary module, Sensors, 22, 2915, 2022.

Schlechtingen, M. and Santos, I. F.: Wind turbine condition monitoring based on SCADA data using normal behavior models. Part 2: Application examples, Applied Soft Computing, 14, 447–460, 2014.

Schlechtingen, M., Santos, I. F., and Achiche, S.: Wind turbine condition monitoring based on SCADA data using normal behavior models. Part 1: System description, Applied Soft Computing, 13, 259–270, 2013.

Schröder, L., Dimitrov, N. K., Verelst, D. R., and Sørensen, J. A.: Using transfer learning to build physics-informed machine learning models for improved wind farm monitoring, Energies, 15, 558, 2022.

Skaare, B., Nielsen, F., Hanson, T., Yttervik, R., Havmoller, O., and Rekdal, A.: Analysis of measurements and simulations from the hywind demo floating wind turbine, Wind Energy, 18, 1105–1122, https://doi.org/10.1002/we.1750, 2014.

Stetco, A., Dinmohammadi, F., Zhao, X., Robu, V., Flynn, D., Barnes, M., Keane, J., and Nenadic, G.: Machine learning methods for wind turbine condition monitoring: A review, Renewable energy, 133, 620–635, 2019.

Tautz-Weinert, J. and Watson, S. J.: Using SCADA data for wind turbine condition monitoring–a review, IET Renewable Power Generation, 11, 382–394, 2017.

Wang, Y., Xiang, J., Markert, R., and Liang, M.: Spectral kurtosis for fault detection, diagnosis and prognostics of rotating machines: A review with applications, Mechanical Systems and Signal Processing, 66, 679–698, 2016.

WindEurope: Wind Energy in Europe: 2021 Statistics and the Outlook for 2022-2026, 2022.

Wu, X., Hou, C., Deng, Z., Fang, C., and Liu, G.: Signal processing of internet of vehicles based on intelligent interference, EURASIP Journal on Advances in Signal Processing, 2022, https://doi.org/10.1186/s13634-022-00864-5, 2022.

Zaher, A., McArthur, S., Infield, D., and Patel, Y.: Online wind turbine fault detection through automated SCADA data analysis, Wind Energy: An International Journal for Progress and Applications in Wind Power Conversion Technology, 12, 574–593, 2009.

Zhao, Y., Zhang, J., Li, J., Liu, S., Miao, P., Shi, Y., and Zhao, E.: A brief review of magnetic anomaly detection, Measurement Science and Technology, 32, 042 002, 2021.